

## Preclinical Development

## Interactions of Tyrosine Kinase Inhibitors with Organic Cation Transporters and Multidrug and Toxic Compound Extrusion Proteins

Tsuyoshi Minematsu and Kathleen M. Giacomini

## Abstract

The drug–drug interaction (DDI) potential of tyrosine kinase inhibitors (TKI) as interacting drugs via transporter inhibition has not been fully assessed. Here, we estimated the half maximal inhibitory concentration (IC<sub>50</sub>) values for 8 small-molecule TKIs (imatinib, dasatinib, nilotinib, gefitinib, erlotinib, sunitinib, lapatinib, and sorafenib) on [<sup>14</sup>C]metformin transport by human organic cation transporters (OCT), OCT1, OCT2, and OCT3, and multidrug and toxic compound extrusion (MATE) proteins, MATE1 and MATE2-K, using human embryonic kidney cells stably expressing these transporters. We then compared the estimated IC<sub>50</sub> values to the maximum clinical concentrations of unbound TKIs in plasma (unbound C<sub>max,sys,p</sub>). Results showed that imatinib, nilotinib, gefitinib, and erlotinib exerted selectively potent inhibitory effects, with unbound C<sub>max,sys,p</sub>/IC<sub>50</sub> values ≥0.1, on MATE1, OCT3, MATE2-K, and OCT1, respectively. In comparison to the common form of OCT1, the OCT1 polymorphism, M420del, was more sensitive to drug inhibition by erlotinib. Major metabolites of several TKIs showed IC<sub>50</sub> values similar to those for unchanged TKIs. Taken together, these findings suggest the potential of clinical transporter-mediated DDIs between specific TKIs and OCTs and MATEs, which may affect the disposition, efficacy, and toxicity of metformin and other drugs that are substrates of these transporters. The study provides the basis for further clinical DDI studies with TKIs. *Mol Cancer Ther*; 10(3); 531–9. ©2011 AACR.

## Introduction

Accumulating evidence highlights the importance of drug transporters in drug disposition, efficacy, and safety, particularly with respect to drug–drug interactions (DDI; ref. 1). A recent review has underscored the need for drug development programs to perform relevant clinical studies of transporter-based DDIs as suggested from *in vitro* studies of drug-transporter interactions (1). In terms of transporter-based DDIs, an interacting drug may be an inhibitor that causes a DDI by inhibition of a transporter's function, or may be a substrate of the transporter. Methodologies and algorithms for predicting transporter-mediated DDIs based on *in vitro* experiments are under discussion (1). A comparison of the concentration of an inhibitor (*I*; generally, the maximum unbound plasma concentration) and its half

maximal inhibitory concentration (IC<sub>50</sub>) for a transporter as determined through *in vitro* studies is performed to determine whether a potential clinical DDI may occur (1). Obviously, high unbound plasma concentrations relative to the IC<sub>50</sub> of the drug is an indicator of a potential clinical DDI. To err on the side of caution, an *I*/IC<sub>50</sub> value ≥0.1 has been suggested as a criterion to use for consideration of conducting a clinical transporter-based DDI (1).

Tyrosine kinase inhibitors (TKI; Supplementary Fig. S1), a new class of anticancer drugs, are rationally designed to target specific tyrosine kinases that are fused, mutated, or overexpressed in cancer (2). In spite of their increasing use, only a few studies have examined the interactions of TKIs with influx transporters and to our knowledge there are no known influx transporter-based clinical DDI between TKIs and other drugs on the market. Most studies examining the interaction of TKIs with influx transporters have focused on substrate rather than inhibition interactions (3–10). Moreover, several TKIs have cationic charge and high lipophilicity (Supplementary Table S1), which are requirements of organic cation transporter, OCT inhibition (11), and therefore have potential to inhibit organic cation transporters, including OCT1 (SLC22A1), OCT2 (SLC22A2), OCT3 (SLC22A3), and MATE1 (SLC47A1) and MATE2-K (SLC47A2). However, to our knowledge, there have been no studies assessing the clinical DDI potential of TKIs.

**Authors' Affiliation:** Department of Bioengineering and Therapeutic Sciences, University of California, San Francisco, California

Note: Supplementary data for this article are available at Molecular Cancer Therapeutics Online (<http://mct.aacrjournals.org/>).

**Corresponding Author:** Kathleen M. Giacomini, Department of Bioengineering and Therapeutic Sciences, University of California, San Francisco, 1550 4th Street, San Francisco, CA 94158. Phone: 415-476-1936; Fax: 415-514-4361; E-mail: [kathy.giacomini@ucsf.edu](mailto:kathy.giacomini@ucsf.edu)

doi: 10.1158/1535-7163.MCT-10-0731

©2011 American Association for Cancer Research.

Drugs from multiple therapeutic classes that are transported by organic cation transporters may be concomitantly used with TKIs. Metformin is recommended as the initial pharmacologic therapy for type 2 diabetes, which is one of the most common diseases in the world. Diabetes and cancer are common conditions, and their codiagnosis in the same individual is not infrequent (12). In humans, OCT1 on the basolateral membrane of hepatocytes is involved in the uptake of metformin from the blood into the liver, which is its major site of pharmacologic action (13, 14). Similarly, OCT2 on the basolateral membrane of renal tubular cells mediates the uptake of metformin from blood into the kidney, which is the major eliminating organ for the drug (15). Recently, MATE1 and MATE2-K on the apical membrane of renal tubular cells have been proposed to act as the final efflux transporters of metformin from the body, namely from renal cells to the urine (16). Several clinical DDIs between metformin and inhibitors of organic cation transporters, such as cimetidine, have been reported (1). Metformin, a typical substrate of OCTs and MATEs, has been extensively studied. Data obtained for metformin may be applicable to other substrates of OCTs and MATEs. Interestingly, metformin has recently been considered a potential candidate in novel treatment strategies for human pancreatic cancer (17) and in combination with lapatinib-based protocols in the treatment of breast cancer (18). Clinical studies of combination therapies of gemcitabine, erlotinib, and metformin in pancreatic cancer and of lapatinib in combination with metformin for various cancers are currently underway (Study ID NCT01210911 and NCT01087983 in <http://clinicaltrials.gov/>). Recently, a clinical case report regarding lactic acidosis induced by a DDI of erlotinib, a TKI, and metformin has been published, but lacks any mention of transporters (19). Because lactic acidosis associated with metformin treatment is a rare but potentially fatal adverse event, this clinical case report underscores the importance of the safe use of metformin in cancer patients. Given that drug transporters are a determinant of metformin pharmacokinetics and pharmacodynamics, possible risks of concomitant use of metformin and TKIs in terms of drug transporters need to be examined. Oxaliplatin, an anticancer platinum analog, is a substrate of organic cation transporters including OCT1, OCT2, and OCT3, which are thought to play a role in its anticancer effects by facilitating its entry into tumor cells (20, 21). Currently, TKIs are being tested in clinical trials in combination with oxaliplatin for the treatment of various tumors (22–25). Moreover, many trials involving oxaliplatin with TKIs are ongoing or completed (<http://clinicaltrials.gov>).

Here, we conducted *in vitro* studies comparing the DDI potential of TKIs on the transport of metformin by OCT1, OCT2, OCT3, MATE1, and MATE2-K to obtain a rationale for clinical DDI studies. We attempted to thoroughly assess the *in vitro* inhibitory effects of 8 small-molecule TKIs (imatinib, dasatinib, nilotinib, gefitinib, erlotinib,

sunitinib, lapatinib, and sorafenib; Supplementary Fig. S1) on transport of metformin by the transporters. For the TKIs that potentially cause clinical DDIs, time-dependent inhibition, genetic variant-mediated alteration of inhibition potency, and inhibition by major metabolites of the drugs were also investigated. Inter-species differences in the transporter inhibition by TKIs were also examined *in vitro* to evaluate the utility of mice as possible surrogate *in vivo* models for assessing clinically relevant transporter-mediated DDI. Relationships between transporter inhibition and physicochemical properties of the TKIs were also determined. In addition, we examined the DDI potential of TKIs with oxaliplatin that may be used in combination with TKIs, and also an important substrate of OCTs and MATEs.

## Materials and Methods

### Drugs and reagents

Imatinib, dasatinib, nilotinib, gefitinib, erlotinib, sunitinib, lapatinib, sorafenib, *N*-desmethyl imatinib, *O*-desmethyl gefitinib, and *O*-desmethyl erlotinib were purchased from Toronto Research Chemical. [<sup>14</sup>C]Metformin was purchased from Moravек Biochemicals and Radiochemicals. Metformin and oxaliplatin were purchased from Sigma-Aldrich. Other reagents and chemicals were purchased from commercial sources.

### Cell lines and transfection

Human embryonic kidney (HEK293) Flp-In-293 cells stably transfected with the full-length reference human *OCT1* cDNA (reference sequence, NM\_003057; HEK-hOCT1), *OCT2* cDNA (HEK-hOCT2), *OCT3* cDNA (HEK-hOCT3), *MATE1* cDNA (HEK-hMATE1), mutant *OCT1* M420del cDNA inserts, and the empty vector (HEK-MOCK) were established previously in our laboratory (13, 21, 26, 27). Stable cell lines expressing recombinant MATE2-K (HEK-hMATE2-K), and mouse Oct1 (HEK-mOct1) were also established previously in our laboratory (unpublished reports). HEK293 cells stably transfected with the full-length reference mouse *Oct2* cDNA (HEK-mOct2), *Oct3* cDNA (HEK-mOct3), and *Mate1* cDNA (HEK-mMate1) were established by transfection of pcDNA5/FRT vector (Invitrogen) containing the full-length transporter cDNA into HEK293 Flp-In-293 cells using Lipofectamine 2000 (Invitrogen) as per the manufacturer's instructions. Stable clones were selected using 75 µg/mL hygromycin B. The general characteristics of all transfected HEK293 cell lines were monitored by checking cell morphology microscopically, and measuring the doubling time of each cell line. The expression level of each transporter mRNA in each transfected HEK293 cell line was verified by real-time RT-PCR method. The transport of metformin and oxaliplatin in transporter-transfected HEK293 cells was compared to that in HEK-MOCK in every transport assay. Authentication of HEK293 Flp-In-293 cells was not performed by the authors.

## Cell culture

Stably transfected HEK293 cells were maintained in Dulbecco's modified eagle medium (DMEM) H-21 medium supplemented with 10% fetal bovine serum, 100 units/mL penicillin, 100 units/mL streptomycin, and 75 µg/mL hygromycin B. All cell lines were grown at 37°C in a humidified atmosphere with 5% CO<sub>2</sub>/95% air.

## Metformin cellular uptake study

The uptake study was performed as described in our previous report with slight modifications (28). Briefly, HEK293 cells were grown on poly-D-lysine-coated 24-well plates in DMEM H-21 medium supplemented with 10% fetal bovine serum to at least 90% confluence (24 hours after seeding). For uptake studies, HEK-MOCK, HEK-hOCT1, HEK-hOCT2, HEK-hOCT3, HEK-mOct1, HEK-mOct2, and HEK-mOct3 were preincubated before the addition of the uptake buffer for 20 minutes with Hank's balanced salt solution (HBSS; 5.4 mmol/L potassium chloride, 0.44 mmol/L monobasic potassium phosphate, 4.2 mmol/L sodium bicarbonate, 137 mmol/L sodium chloride, 0.34 mmol/L dibasic sodium phosphate, 5.6 mmol/L D-glucose, 1.3 mmol/L calcium chloride, 0.49 mmol/L magnesium chloride, 0.41 mmol/L magnesium sulfate, pH 7.4), and then incubated in the uptake buffer (HBSS containing 10 µmol/L unlabeled and [<sup>14</sup>C]-labeled metformin). Uptake was performed at 37°C for the designated period of time for which linear uptake was observed, and then the cells were washed twice with ice-cold HBSS. The cells were lysed with 0.1 N NaOH and 0.1% SDS, and the lysate was used for scintillation counting (Beckman Coulter) and for the bicinchoninic acid protein assay (Pierce). For uptake by MATE, HEK-MOCK, HEK-hMATE1, HEK-hMATE2-K, and HEK-mMate1, cells were preincubated before the uptake study with HBSS (pH 7.4) in the presence of 30 mmol/L ammonium chloride for 20 minutes (16). The preincubation medium was then removed, and the cells were incubated with uptake medium containing [<sup>14</sup>C]metformin in the same manner as for OCTs.

## Cellular accumulation of platinum

The cellular accumulation of platinum was determined after 2-hour exposure to oxaliplatin as previously described (21), with slight modification. Briefly, HBSS (pH 7.4) was used as the uptake buffer, and the platinum content in the cells was determined by inductively coupled plasma mass spectrometry in the Analytical Facility at University of California, Santa Cruz. Cellular platinum accumulation was normalized to the protein content determined via bicinchoninic acid protein assay.

## Data analysis

**Determination of IC<sub>50</sub> values.** Half-maximal IC<sub>50</sub> values were calculated by simultaneously fitting the data in transporter-expressing cells and mock cells, without a

weighting factor, to the following equations (29) using WinNonlin:

$$CL_{\text{uptake,+inh}} = (CL_{\text{uptake}} - P_{\text{dif}})/(1+[I]/IC_{50}) + P_{\text{dif}} \text{ (for transporter-expressing cells)}$$

$$CL_{\text{uptake,+inh}} (= CL_{\text{uptake}}) = P_{\text{dif}} \text{ (for mock cells)}$$

where CL<sub>uptake</sub> is the uptake clearance (µL/min/mg protein) in the absence of inhibitor, CL<sub>uptake,+inh</sub> is that in the presence of inhibitor, [I] is the inhibitor concentration, and P<sub>dif</sub> is the component of passive diffusion (µL/min/mg protein). Given that the substrate concentration in the inhibition study was low compared with the Michaelis-Menten constant K<sub>m</sub>, the IC<sub>50</sub> values are virtually equal to the inhibition constant K<sub>i</sub> values, assuming competitive or noncompetitive inhibition (1). Each set of [I] consists of 0 and 6 concentrations, so that each IC<sub>50</sub> value was within the concentration range used in the studies.

**Clinical concentrations of TKIs.** Maximum clinical concentrations of unbound TKIs in systemic plasma (C<sub>max,sys,p</sub>) and unbound fraction in plasma were obtained from the literature (Supplementary Table S1; refs. 30-38). Absorption rate constants (k<sub>a</sub>) were calculated using the reported time to reach C<sub>max,sys,p</sub> (T<sub>max</sub>) and half life (t<sub>1/2</sub>; ref. 30), and the following equation (39):

$$T_{\text{max}} = [\ln(k_a/k_{\text{el}})]/(k_a - k_{\text{el}}), k_{\text{el}} = \ln 2/t_{1/2}$$

where k<sub>el</sub> is the elimination rate constant, assuming a monoexponential decline of plasma levels of drug with first order absorption and k<sub>a</sub> > k<sub>el</sub>. If k<sub>a</sub> was calculated to be greater than 0.1/min, then it was fixed at 0.1/min (39). Clinical maximum concentration of unbound TKI in portal plasma (unbound C<sub>max,portal,p</sub>) was calculated using the following equation (39):

$$C_{\text{max,portal,p}} = f_{\text{u,p}} \cdot C_{\text{max,p,sys}} + (f_{\text{u,p}}/R_b) \cdot \text{Dose} \cdot F_a \cdot F_g \cdot k_a/Q_h$$

where f<sub>u,p</sub> is the unbound fraction in plasma, R<sub>b</sub> is the blood-to-plasma concentration ratio, F<sub>a</sub> and F<sub>g</sub> are bioavailability via the first-pass effect in absorption and intestinal metabolism, respectively, and Q<sub>h</sub> is hepatic blood flow rate (1,500 mL/min; ref. 1). F<sub>a</sub>, F<sub>g</sub>, and R<sub>b</sub> were assumed to be 1 in the present study.

**Relationship between physicochemical properties of TKIs and transporter inhibition potency.** Charge at pH 7.4 and lipophilicity parameters (calculated octanol-water partition coefficient, C log P, and calculated octanol-water distribution coefficient at pH 7.4, C log D<sub>pH7.4</sub>) of TKIs were calculated using the software Marvin View (ChemAxon Kft.; Supplementary Table S1). Other physicochemical parameters, H-bond donor count, H-bond acceptor count, rotatable bond count, tautomer count, molecular weight, topological polar surface area, heavy atom count, and complexity, were obtained from PubChem (<http://pubchem.ncbi.nlm.nih.gov>). PubChem is an open repository for experimental data identifying the biological activities of small molecules, which includes computed properties of the compound record (40). The IC<sub>50</sub> values of

TKIs in inhibiting metformin uptake via human OCTs and MATEs (Supplementary Table S2) were expressed in mol/L, transformed into logarithm, and then multiplied by  $-1$ , i.e., negative  $\log_{10}(\text{IC}_{50})$  values, so that higher values equate to higher inhibitory effects. In cases in which the  $\text{IC}_{50}$  value was  $>30 \mu\text{mol/L}$ , negative  $\log_{10}(\text{IC}_{50})$  was assumed to be  $-\log_{10}(3 \times 10^{-6})$ . Pearson's correlation coefficient ( $R$ ) and  $P$  value (two-tailed) between physicochemical parameters and negative  $\log_{10}(\text{IC}_{50})$  values were calculated using GraphPad Prism (GraphPad Software, Inc.), after confirmation of normality of data distribution by D'Agostino and Pearson omnibus normality test.

## Results

### TKIs, at clinically relevant concentrations, inhibit the transport of metformin by OCTs and MATEs

The  $\text{IC}_{50}$  values of the 7 TKIs against, OCT1, OCT2, OCT3, MATE1, and MATE2-K are shown in Supplementary Table S2. Of note, most of the TKIs including imatinib, dasatinib, nilotinib, gefitinib, and sunitinib were potent inhibitors of the transporters, with  $\text{IC}_{50}$  values generally in the low micromolar range. Lapatinib and sorafenib, in contrast, were poor inhibitors of [ $^{14}\text{C}$ ]metformin uptake by the transporters. Comparison of the unbound  $C_{\text{max,sys,p}}$  (Supplementary Table S1) and  $\text{IC}_{50}$  values of TKIs against human OCT1, OCT2, OCT3, MATE1, and MATE2-K (Supplementary Table S2) showed that imatinib (for OCT1, hMATE1, and MATE2K), nilotinib (for OCT3), gefitinib (for MATE2K), and erlotinib (for OCT1 and MATE2K) exerted potent inhibitory effects at clinically relevant concentrations, with  $[I]/\text{IC}_{50} \geq 0.1$  using unbound  $C_{\text{max,sys,p}}$  as  $[I]$  (Fig. 1). If unbound maximum concentrations in the portal vein,  $C_{\text{max,portal,p}}$  (Supplementary Table S1) were used as  $[I]$  for the liver transporter (hOCT1), several of the TKIs (imatinib, dasatinib, gefitinib, and sunitinib) were predicted to inhibit metformin uptake into the liver at concentrations in the hepatic sinusoids that may be observed after oral doses of the drugs.

### Other factors such as genetic polymorphisms and preincubation modulate inhibition potencies of TKIs

Because erlotinib was a potent inhibitor of OCT1 at clinically relevant concentrations, we studied its potency as an inhibitor of a common polymorphism of OCT1, M420del, which has reduced function with respect to metformin uptake. Our findings showed that erlotinib exerted a more potent inhibitory effect on the polymorphism than it did on the reference OCT1 (Fig. 2). Further, erlotinib showed an even more potent inhibitory effect on metformin transport by the reference OCT1 after preincubation with cells before initiating the uptake reaction (Fig. 3).

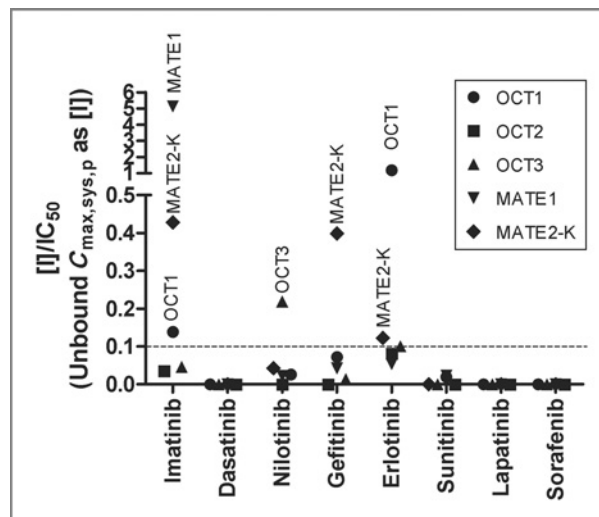


Figure 1. Unbound  $[I]/\text{IC}_{50}$  values for tyrosine kinase inhibitors as inhibitors of human OCT1, OCT2, OCT3, MATE1, and MATE2-K. Unbound  $C_{\text{max,sys,p}}$  values representing  $[I]$ , shown in Supplementary Table S1 and  $\text{IC}_{50}$  values from Supplementary Table S2 were used in to calculate  $[I]/\text{IC}_{50}$ . The broken line represents  $[I]/\text{IC}_{50} = 0.1$ .

### Major metabolites of TKIs inhibit the transport of metformin by OCTs and MATEs

*N*-desmethyl imatinib and *O*-desmethyl gefitinib, which are major metabolites of imatinib and gefitinib, respectively, showed inhibition properties similar to those of imatinib (potent and selective inhibition of MATE1) and gefitinib (potent and selective inhibition of MATE2-K; Supplementary Table S3). In contrast, *O*-desmethyl erlotinib, a major metabolite of erlotinib, was not a potent inhibitor of OCT1 (Supplementary Table S3) as was the parent compound (Supplementary Table S2).

### Great inter-species differences in inhibition potencies of imatinib, nilotinib, and erlotinib for human and mouse OCTs and MATEs are observed

We noted large differences in  $\text{IC}_{50}$  values and selectivity of inhibition of TKIs between human and mouse transporter orthologs (Fig. 4). In particular, imatinib, nilotinib, and erlotinib exerted less potent inhibition of mouse transporters mMate1, mOct3 and mOct1, respectively, in comparison to the human orthologs.

### Cellular uptake of oxaliplatin in the presence of erlotinib and nilotinib

To determine whether erlotinib and nilotinib would inhibit oxaliplatin uptake at concentrations in the range of clinically achieved unbound concentrations in plasma, we tested  $2 \mu\text{mol/L}$  as the highest concentration. Cellular platinum uptake after incubation of HEK-hOCT1, -hOCT2, and -hOCT3 with oxaliplatin ( $2 \mu\text{mol/L}$  for 2 hours) was decreased in the presence of erlotinib and nilotinib in a concentration-dependent manner (Fig. 5). Erlotinib and nilotinib showed potent uptake inhibition

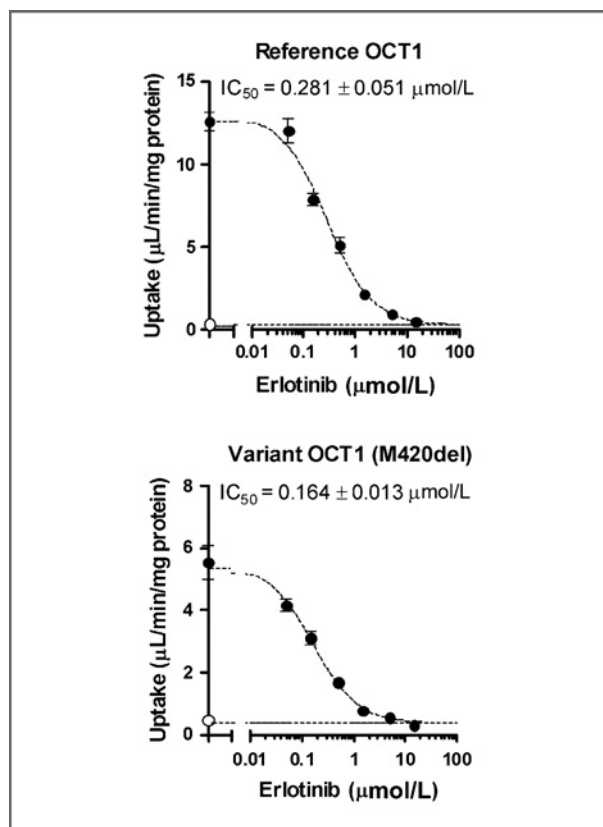


**Figure 2.** Inhibitory effects of erlotinib on the uptake of [<sup>14</sup>C]metformin (10 μmol/L for 5 minutes) by human OCT1 reference and variant (M420del). Closed symbols represent the uptake of metformin into HEK-hOCT1 reference and HEK-hOCT1 M420del, and open symbols represent the uptake into HEK-MOCK cells. Data are expressed as mean ± SD (*n* = 3).

of HEK-hOCT1 and HEK-hOCT3, respectively, between transporter-expressing HEK cells.

### Relationship between physicochemical properties of TKIs and transporter inhibition potency

Lipophilicity parameters,  $C \log P$  and  $C \log D_{pH7.4}$ , correlated negatively with negative  $\log_{10}(IC_{50})$  of TKIs for human OCT1 and OCT2 (Fig. 6). With regard to human MATE1, the charge at pH7.4 correlated positively with negative  $\log_{10}(IC_{50})$  values (Fig. 6). For OCT3 and MATE2-K, lipophilicity or charge did not significantly correlate with negative  $\log_{10}(IC_{50})$  [data not shown]. In addition, for all tested transporters, there was no significant correlation between negative  $\log_{10}(IC_{50})$  values and the parameters of H-bond donor count, H-bond acceptor count, rotatable bond count, tautomer count, molecular weight, topological polar surface area, heavy atom count, and complexity (data not shown).

### Discussion

Here, we investigated the possibility of clinical DDIs via inhibitory effects of 8 small-molecule TKIs on the

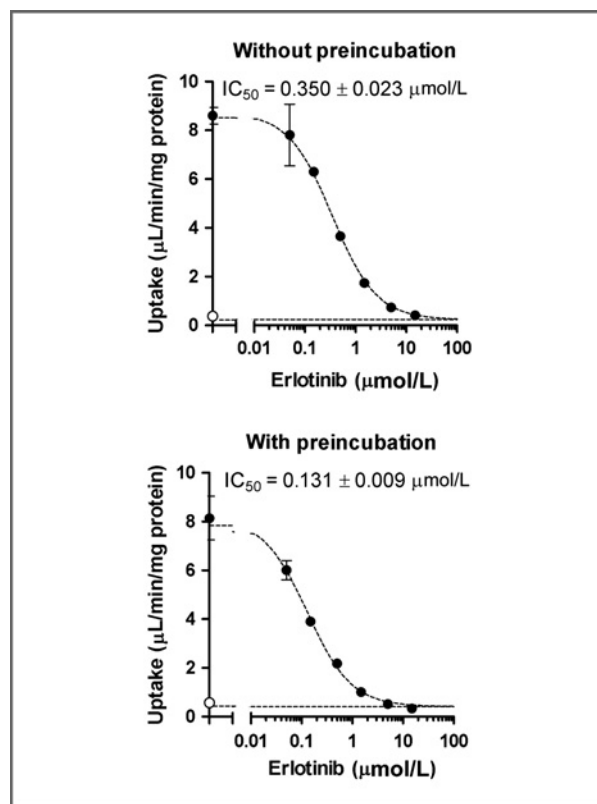


**Figure 3.** The effect of preincubation on the inhibitory effects of erlotinib on the uptake of [<sup>14</sup>C]metformin (10 μmol/L for 5 minutes) by human OCT1. Closed symbols represent the uptake of metformin into HEK-hOCT1, and open symbols represent the uptake into HEK-MOCK cells. Data are expressed as mean ± SD (*n* = 3).

transport activity of human OCT1, OCT2, OCT3, MATE1, and MATE2-K. Our results showed that imatinib, nilotinib, gefitinib, and erlotinib exerted selectively potent inhibitory effects with unbound  $C_{max,sys,p}/IC_{50} \geq 0.1$  on MATE1, OCT3, MATE2-K, and OCT1, respectively. In particular, unbound  $C_{max,sys,p}/IC_{50}$  was greater than 1 for the inhibition of MATE1 by imatinib and of OCT1 by erlotinib, suggesting a high probability of a DDI if the compounds are administered with metformin.

Because drug concentrations at the inlet of the liver after oral administration are generally expected to be higher than in the systemic circulation (39), actual risks of DDI may be underestimated by unbound  $C_{max,sys,p}/IC_{50}$ . Therefore, unbound  $C_{max,portal,p}$  values (Supplementary Table S1; ref. 39) may be used as  $[I]$  to predict potential DDIs with transporters in the liver (hOCT1) to avoid false-negative predictions. Prevalence of type 2 diabetes ranges from 2% to 10% in industrialized countries, with rates on the rise (41). Because cancer and type 2 diabetes are 2 common diseases that may share risk factors (41), many present and future patients will likely undergo concomitant treatment with TKIs and metformin. Importantly, because metformin appears to have

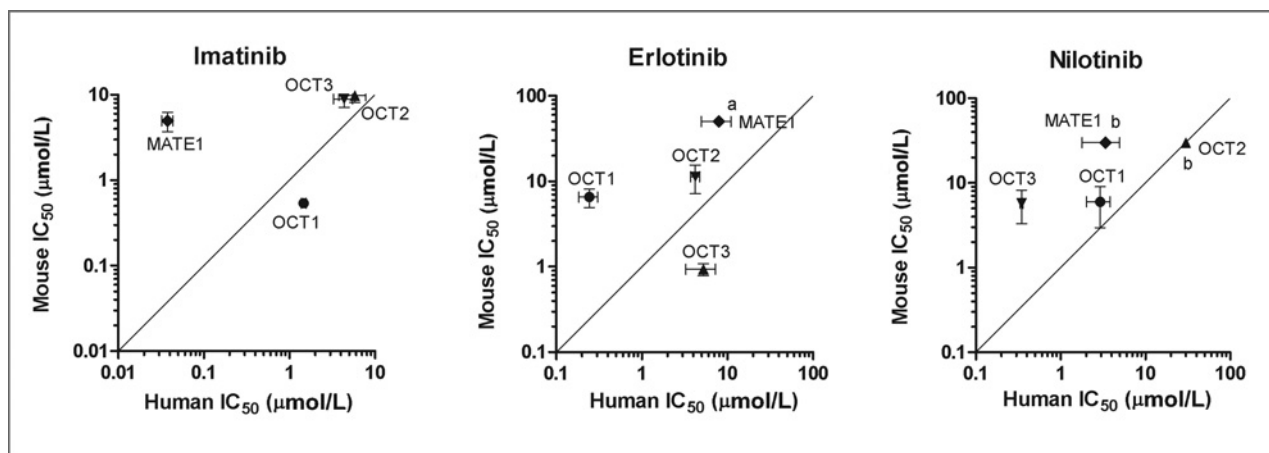


Figure 4. Interspecies differences in the inhibition potencies (IC<sub>50</sub> values) for imatinib, nilotinib, and erlotinib between human and mouse orthologs of OCT1-3, and MATE1. a, the actual IC<sub>50</sub> value was estimated to be >50 µmol/L for mouse MATE1. b, the actual IC<sub>50</sub> value was estimated to be >30 µmol/L for mouse OCT2 and MATE1 and human OCT2. A solid line represents the line of the unity.

some efficacy in cancer management, clinical studies with TKIs and metformin are ongoing. Though relatively safe, at high concentrations, metformin can cause lactic acidosis, a life-threatening adverse reaction. DDIs with TKIs may result in increased levels of metformin and therefore, increase patient susceptibility to lactic acidosis. Such DDIs may be particularly problematic in patients with widespread metastases who are at increased risk for lactic acidosis. Our study strongly supports the need for clinical DDI studies between metformin and TKIs.

Methods used in the *in vitro* assessment of drug transporter interactions are important to obtain accurate predictions of potential clinical DDIs. The current standard *in vitro* method of evaluating a drug as an inhibitor

of an uptake transporter involves simultaneous addition of the test drug inhibitor and model substrate and determination of uptake of the substrate. In real clinical situations, however, a drug may be metabolized into several distinct chemical species, and the transporter may be exposed to the inhibitor drug for a long period of time before a substrate is administered (28). We found that preincubation of erlotinib with the cells before initiation of metformin uptake enhanced the inhibitory effects of erlotinib on OCT1 (Fig. 3). This suggests that the interaction of erlotinib with the lipophilic and negatively charged cell membrane, which is supposed to be crucial step in achieving OCT1 inhibition (11), or other steps required for erlotinib to reach its binding domain on OCT1 may be slow. We also

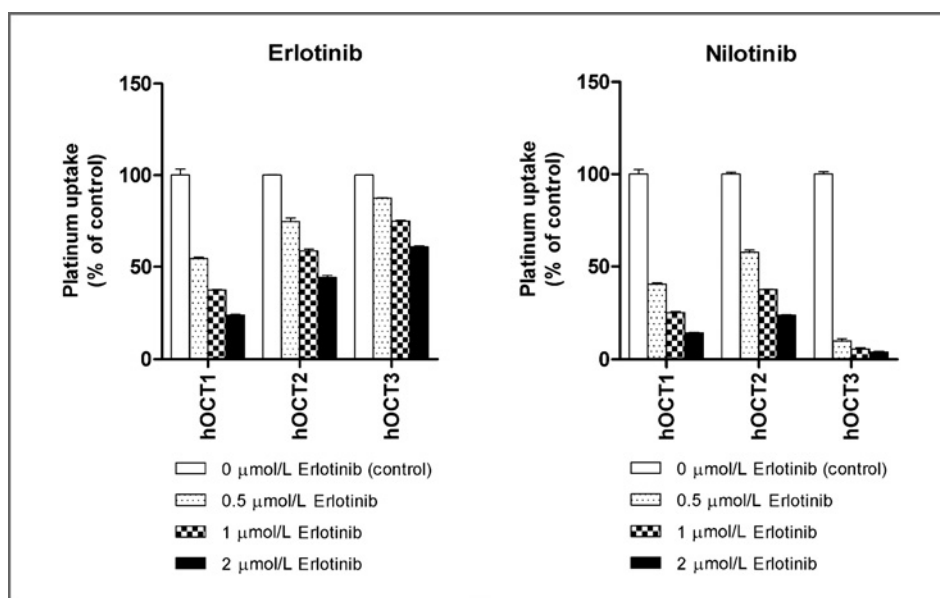
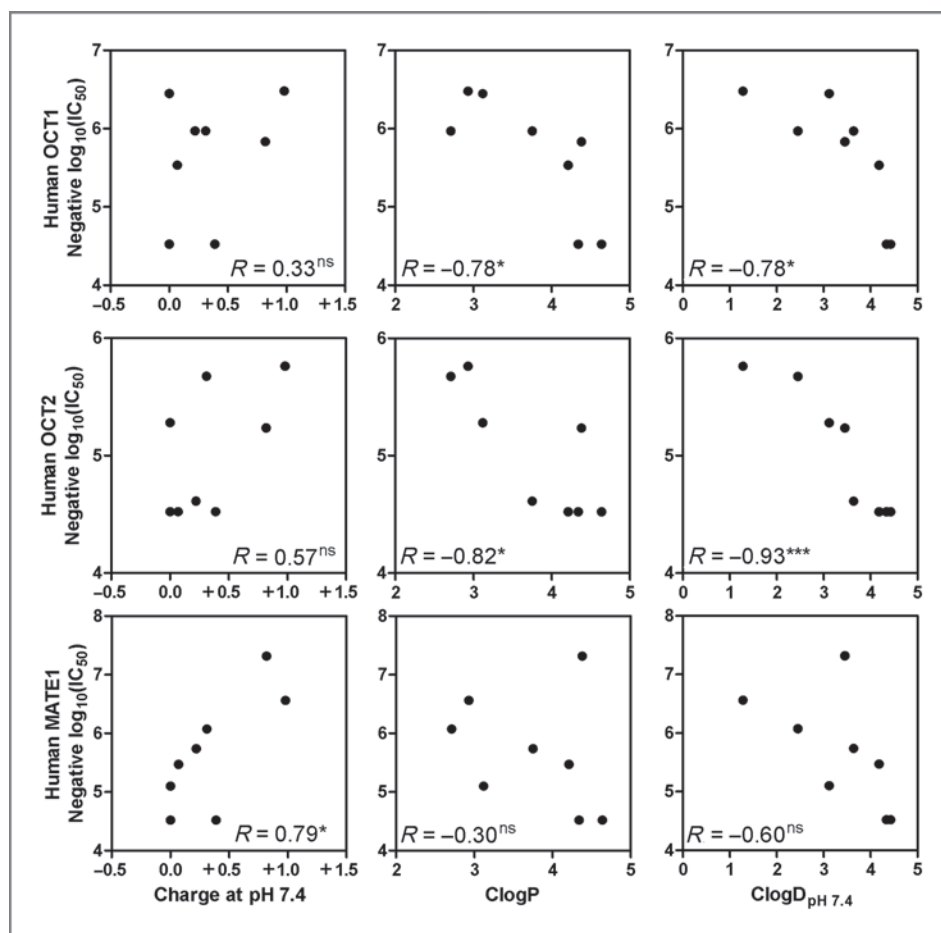


Figure 5. Cellular platinum uptake into HEK-hOCT1, -hOCT2, and -hOCT3 after 2-hour incubation with oxaliplatin (2 µmol/L) in the absence and presence of erlotinib and nilotinib. The results are expressed as transporter-specific uptake, subtracting the uptake into HEK-hOCT1, -hOCT2, and -hOCT3 by that into HEK-MOCK. Data are expressed as mean ± SD (n = 3).

Figure 6. Correlation between physicochemical properties of TKIs and negative  $\log_{10}(\text{IC}_{50})$  for human OCT1, OCT2 and MATE1. Pearson's  $R$  and  $P$  values were calculated (<sup>ns</sup> $P \geq 0.05$ , \* $P < 0.05$ , and \*\*\* $P < 0.001$ ).



observed that the inhibition potency of erlotinib was increased for the M420del (Fig. 2), a common polymorphism of OCT1 found at allele frequencies of about 20% in white Americans (13). Our data are consistent with a previous study showing that M420del is more sensitive to drug inhibition by glibenclamide, simvastatin, and verapamil, with  $\text{IC}_{50}$  values up to 8 times lower for the variant than those observed for the reference OCT1 (28).

Major metabolites of TKIs showed  $\text{IC}_{50}$  values similar to those for unchanged TKIs. Plasma concentrations of *O*-desmethyl gefitinib in CYP2D6 extensive metabolizers are higher than for unchanged gefitinib (42). Therefore, *O*-desmethyl gefitinib may contribute to potential clinical DDIs that may occur following concomitant metformin and gefitinib administration. Given that plasma concentrations of *N*-desmethyl imatinib are approximately 10-fold lower than those of the unchanged imatinib (43), and the unbound fractions of *N*-desmethyl imatinib and imatinib are nearly equal (44), the inhibitory effects of *N*-desmethyl imatinib on the tested transporters may be negligible at therapeutic doses of imatinib. *O*-desmethyl erlotinib is a 10-fold weaker inhibitor of OCT1 than erlotinib (Supplementary Table S3), and the metabolite

concentration in plasma is more than 10-fold lower than that of the unchanged erlotinib (45), suggesting little inhibitory effects at normal doses.

To determine whether mice could be used as animal models to study transporter-based human DDIs between TKIs and OCTs and MATEs, we investigated the inhibition potency of TKIs for mouse orthologs of OCTs and MATEs. Our data showed striking species differences in the interaction of erlotinib, nilotinib, and imatinib, with mouse orthologs of OCT1, OCT3, and MATE1, respectively, in comparison to the human orthologs (Fig. 4). All 3 compounds had weaker interactions with the mouse transporters in comparison to the human orthologs. This finding suggests that mice are unlikely to be suitable animal models for *in vivo* DDI studies of TKIs and OCTs/MATEs. The structural basis for the reduced potency of interaction of the TKIs with the mouse orthologs of the transporters is not known and needs investigation. Because high resolution crystal structures of OCTs and MATEs are not available for construction of molecular models, it is difficult to explain the structural basis for the striking interspecies differences that were observed in the interaction of TKIs with OCTs and MATEs.

In this study, we observed that the cellular uptake of platinum was reduced after oxaliplatin treatment in the presence of clinically relevant concentrations of erlotinib and nilotinib (Fig. 5). These experiments suggest that combination therapy involving oxaliplatin and these TKIs may not be optimal, particularly for tumors in which OCTs are involved in the uptake of oxaliplatin. Coadministration of erlotinib or nilotinib may reduce the anticancer effects of oxaliplatin by inhibiting the drug's uptake into such tumors. Nilotinib appears to be a more potent inhibitor of oxaliplatin transport by hOCT1, hOCT2, and hOCT3 than of metformin transport. This may suggest that the inhibition potency of TKIs on OCTs may be different depending on the substrate and/or that experimental condition such as incubation time may affect the results of *in vitro* assessment.

Negative correlations between lipophilicity ( $C \log P$  and  $C \log D_{pH7.4}$ ) and negative  $\log_{10}(IC_{50})$  of the TKIs for human OCT1 and OCT2 (Fig. 6) suggest that excessive lipophilicity weakens the inhibitory effects of TKIs on metformin uptake by OCT1 and OCT2. These data are not in agreement with studies demonstrating that high lipophilicity is one of the key physicochemical properties for OCT1 inhibition (11). Excessive lipophilicity may make it difficult for a drug to access the substrate binding region of OCT1 that is in contact with the aqueous phase (46).  $C \log P$  values of the tested TKIs (Supplementary Table S1) met the minimum requirement of lipophilicity needed for OCT1

inhibition (11). Our study also suggests that positive charge may be one of key factors for MATE1 inhibition (Fig. 6). Because the number of tested compounds is small, further studies are needed for accurate drug-structure-based prediction of transporter inhibitory effects.

In the present study, we investigated the possibility of clinical DDIs in response to the inhibitory effects of 8 small-molecule TKIs on the transport activity of human OCT1, OCT2, OCT3, MATE1, and MATE2-K. Results showed the potential for clinical DDIs when certain TKIs were used concomitantly with drugs that are transported by organic cation transporters such as metformin or oxaliplatin. The results of this study provide the basis for further clinical studies investigating the transporter-based DDI potential of TKIs.

### Disclosure of Potential Conflicts of Interest

No potential conflicts of interest were disclosed.

### Grant Support

This work was supported by National Institutes of Health (NIH) Grants GM36780 and GM074929.

The costs of publication of this article were defrayed in part by the payment of page charges. This article must therefore be hereby marked *advertisement* in accordance with 18 U.S.C. Section 1734 solely to indicate this fact.

Received August 5, 2010; revised October 13, 2010; accepted November 22, 2010; published OnlineFirst January 20, 2011.

### References

- Giacomini KM, Huang SM, Tweedie DJ, Benet LZ, Brouwer KL, Chu X, et al. Membrane transporters in drug development. *Nat Rev Drug Discov* 2010;9:215–36.
- Hartmann JT, Haap M, Kopp HG, Lipp HP. Tyrosine kinase inhibitors—a review on pharmacology, metabolism and side effects. *Curr Drug Metab* 2009;10:470–81.
- Hu S, Chen Z, Franke R, Orwick S, Zhao M, Rudek MA, et al. Interaction of the multikinase inhibitors sorafenib and sunitinib with solute carriers and ATP-binding cassette transporters. *Clin Cancer Res* 2009;15:6062–9.
- Thomas J, Wang L, Clark RE, Pirmohamed M. Active transport of imatinib into and out of cells: implications for drug resistance. *Blood* 2004;104:3739–45.
- Davies A, Jordanides NE, Giannoudis A, Lucas CM, Hatzieremia S, Harris RJ, et al. Nilotinib concentration in cell lines and primary CD34(+) chronic myeloid leukemia cells is not mediated by active uptake or efflux by major drug transporters. *Leukemia* 2009;23:1999–2006.
- Hu S, Franke RM, Filipski KK, Hu C, Orwick SJ, de Bruijn EA, et al. Interaction of imatinib with human organic ion carriers. *Clin Cancer Res* 2008;14:3141–8.
- Hiwase DK, Saunders V, Hewett D, Frede A, Zrim S, Dang P, et al. Dasatinib cellular uptake and efflux in chronic myeloid leukemia cells: therapeutic implications. *Clin Cancer Res* 2008;14:3881–8.
- Giannoudis A, Davies A, Lucas CM, Harris RJ, Pirmohamed M, Clark RE. Effective dasatinib uptake may occur without human organic cation transporter 1 (hOCT1): implications for the treatment of imatinib-resistant chronic myeloid leukemia. *Blood* 2008;112:3348–54.
- Polli JW, Humphreys JE, Harmon KA, Castellino S, O'Mara MJ, Olson KL, et al. The role of efflux and uptake transporters in [N-(3-chloro-4-[[3-fluorobenzyl]oxy]phenyl)-6-[5-[[[2-(methylsulfonyl)ethyl]amino]methyl]-2-furyl]-4-quinazolinamine (GW572016, lapatinib) disposition and drug interactions. *Drug Metab Dispos* 2008;36:695–701.
- Tanihara Y, Masuda S, Katsura T, Inui K. Protective effect of concomitant administration of imatinib on cisplatin-induced nephrotoxicity focusing on renal organic cation transporter OCT2. *Biochem Pharmacol* 2009;78:1263–71.
- Ahlin G, Karlsson J, Pedersen JM, Gustavsson L, Larsson R, Mattsson P, et al. Structural requirements for drug inhibition of the liver specific human organic cation transport protein 1. *J Med Chem* 2008;51:5932–42.
- Chowdhury TA. Diabetes and cancer. *QJM* 2010;103:905–15.
- Shu Y, Sheardown SA, Brown C, Owen RP, Zhang S, Castro RA, et al. Effect of genetic variation in the organic cation transporter 1 (OCT1) on metformin action. *J Clin Invest* 2007;117:1422–31.
- Shu Y, Brown C, Castro RA, Shi RJ, Lin ET, Owen RP, et al. Effect of genetic variation in the organic cation transporter 1, OCT1, on metformin pharmacokinetics. *Clin Pharmacol Ther* 2008;83:273–80.
- Chen Y, Li S, Brown C, Cheatham S, Castro RA, Leabman MK, et al. Effect of genetic variation in the organic cation transporter 2 on the renal elimination of metformin. *Pharmacogenet Genomics* 2009;19:497–504.
- Tanihara Y, Masuda S, Sato T, Katsura T, Ogawa O, Inui K. Substrate specificity of MATE1 and MATE2-K, human multidrug and toxin extrusions/H(+)–organic cation antiporters. *Biochem Pharmacol* 2007;74:359–71.
- Kisfalvi K, Eibl G, Sinnott-Smith J, Rozengurt E. Metformin disrupts crosstalk between G protein-coupled receptor and insulin receptor signaling systems and inhibits pancreatic cancer growth. *Cancer Res* 2009;69:6539–45.



18. Vazquez-Martin A, Oliveras-Ferraro C, del Barco S, Martin-Castillo B, Menendez JA. mTOR inhibitors and the anti-diabetic biguanide metformin: new insights into the molecular management of breast cancer resistance to the HER2 tyrosine kinase inhibitor lapatinib (Tykerb). *Clin Transl Oncol* 2009;11:455–9.
19. Pellegrinotti M, Fimognari FL, Franco A, Repetto L, Pastorelli R. Erlotinib-induced hepatitis complicated by fatal lactic acidosis in an elderly man with lung cancer. *Ann Pharmacother* 2009;43:542–5.
20. Yokoo S, Masuda S, Yonezawa A, Terada T, Katsura T, Inui K. Significance of organic cation transporter 3 (SLC22A3) expression for the cytotoxic effect of oxaliplatin in colorectal cancer. *Drug Metab Dispos* 2008;36:2299–306.
21. Zhang S, Lovejoy KS, Shima JE, Lagpacan LL, Shu Y, Lapuk A, et al. Organic cation transporters are determinants of oxaliplatin cytotoxicity. *Cancer Res* 2006;66:8847–57.
22. Pectasides D, Nikolaou M, Pectasides E, Koumariou A, Valavanis C, Economopoulos T. Complete response after imatinib mesylate administration in a patient with chemoresistant stage IV seminoma. *Anticancer Res* 2008;28:2317–20.
23. Van Cutsem E, Verslype C, Beale P, Clarke S, Bugat R, Rakhit A, et al. A phase Ib dose-escalation study of erlotinib, capecitabine and oxaliplatin in metastatic colorectal cancer patients. *Ann Oncol* 2008;19:332–9.
24. Fisher GA, Kuo T, Ramsey M, Schwartz E, Rouse RV, Cho CD, et al. A phase II study of gefitinib, 5-fluorouracil, leucovorin, and oxaliplatin in previously untreated patients with metastatic colorectal cancer. *Clin Cancer Res* 2008;14:7074–9.
25. Kopetz S, Lesslie DP, Dallas NA, Park SI, Johnson M, Parikh NU, et al. Synergistic activity of the SRC family kinase inhibitor dasatinib and oxaliplatin in colon carcinoma cells is mediated by oxidative stress. *Cancer Res* 2009;69:3842–9.
26. More SS, Li S, Yee SW, Chen L, Xu Z, Jablons DM, et al. Organic cation transporters modulate the uptake and cytotoxicity of picoplatin, a third-generation platinum analogue. *Mol Cancer Ther* 2010;9:1058–69.
27. Chen Y, Zhang S, Sorani M, Giacomini KM. Transport of paraquat by human organic cation transporters and multidrug and toxic compound extrusion family. *J Pharmacol Exp Ther* 2007;322:695–700.
28. Ahlin G, Chen L, Lazorova L, Chen Y, Ianculescu AG, Davis RL, et al. Genotype-dependent effects of inhibitors of the organic cation transporter, OCT1: predictions of metformin interactions. *Pharmacogenomics J* 2010. in press.
29. Minematsu T, Hashimoto T, Aoki T, Usui T, Kamimura H. Role of organic anion transporters in the pharmacokinetics of zonampanel, an alpha-amino-3-hydroxy-5-methylisoxazole-4-propionate receptor antagonist, in rats. *Drug Metab Dispos* 2008;36:1496–504.
30. van Erp NP, Gelderblom H, Guchelaar HJ. Clinical pharmacokinetics of tyrosine kinase inhibitors. *Cancer Treat Rev* 2009;35:692–706.
31. le Coutre P, Kreuzer KA, Pursche S, Bonin M, Leopold T, Baskaynak G, et al. Pharmacokinetics and cellular uptake of imatinib and its main metabolite CGP74588. *Cancer Chemother Pharmacol* 2004;53:313–23.
32. Demetri GD, Lo Russo P, MacPherson IR, Wang D, Morgan JA, Branton VG, et al. Phase I dose-escalation and pharmacokinetic study of dasatinib in patients with advanced solid tumors. *Clin Cancer Res* 2009;15:6232–40.
33. Tanaka C, Yin OQ, Sethuraman V, Smith T, Wang X, Grouss K, et al. Clinical pharmacokinetics of the BCR-ABL tyrosine kinase inhibitor nilotinib. *Clin Pharmacol Ther* 2010;87:197–203.
34. Nakagawa K, Tamura T, Negoro S, Kudoh S, Yamamoto N, Yamamoto N, et al. Phase I pharmacokinetic trial of the selective oral epidermal growth factor receptor tyrosine kinase inhibitor gefitinib ('Iressa', ZD1839) in Japanese patients with solid malignant tumors. *Ann Oncol* 2003;14:922–30.
35. Yamamoto N, Horiike A, Fujisaka Y, Murakami H, Shimoyama T, Yamada Y, et al. Phase I dose-finding and pharmacokinetic study of the oral epidermal growth factor receptor tyrosine kinase inhibitor Ro50–8231 (erlotinib) in Japanese patients with solid tumors. *Cancer Chemother Pharmacol* 2008;61:489–96.
36. Shirao K, Nishida T, Doi T, Komatsu Y, Muro K, Li Y, et al. Phase I/II study of sunitinib malate in Japanese patients with gastrointestinal stromal tumor after failure of prior treatment with imatinib mesylate. *Invest New Drugs* 2010;28:866–75.
37. Nakagawa K, Minami H, Kanazaki M, Mukaiyama A, Minamide Y, Uejima H, et al. Phase I dose-escalation and pharmacokinetic trial of lapatinib (GW572016), a selective oral dual inhibitor of ErbB-1 and -2 tyrosine kinases, in Japanese patients with solid tumors. *Jpn J Clin Oncol* 2009;39:116–23.
38. Okamoto I, Miyazaki M, Morinaga R, Kaneda H, Ueda S, Hasegawa Y, et al. Phase I clinical and pharmacokinetic study of sorafenib in combination with carboplatin and paclitaxel in patients with advanced non-small cell lung cancer. *Invest New Drugs* 2010;28:844–53.
39. Ito K, Iwatsubo T, Kanamitsu S, Ueda K, Suzuki H, Sugiyama Y. Prediction of pharmacokinetic alterations caused by drug-drug interactions: metabolic interaction in the liver. *Pharmacol Rev* 1998;50:387–412.
40. Bolton E, Wang Y, Thiessen P, Bryant S. PubChem: Integrated platform of small molecules and biological activities. In: Wheeler RA, Spellmeyer D, editors. *Annual Reports in Computational Chemistry*. Vol 4. Oxford, UK; 2008. Chapter 12:217–41.
41. Hemminki K, Li X, Sundquist J, Sundquist K. Risk of cancer following hospitalization for type 2 diabetes. *Oncologist* 2010;15:548–55.
42. Swaisland HC, Cantarini MV, Fuhr R, Holt A. Exploring the relationship between expression of cytochrome P450 enzymes and gefitinib pharmacokinetics. *Clin Pharmacokinet* 2006;45:633–44.
43. Gschwind HP, Pfaar U, Waldmeier F, Zollinger M, Sayer C, Zbinden P, et al. Metabolism and disposition of imatinib mesylate in healthy volunteers. *Drug Metab Dispos* 2005;33:1503–12.
44. Kretz O, Weiss HM, Schumacher MM, Gross G. In vitro blood distribution and plasma protein binding of the tyrosine kinase inhibitor imatinib and its active metabolite, CGP74588, in rat, mouse, dog, monkey, healthy humans and patients with acute lymphatic leukaemia. *Br J Clin Pharmacol* 2004;58:212–6.
45. Frohna P, Lu J, Eppler S, Hamilton M, Wolf J, Rakhit A, et al. Evaluation of the absolute oral bioavailability and bioequivalence of erlotinib, an inhibitor of the epidermal growth factor receptor tyrosine kinase, in a randomized, crossover study in healthy subjects. *J Clin Pharmacol* 2006;46:282–90.
46. Popp C, Gorboulev V, Muller TD, Gorbunov D, Shatskaya N, Koepsell H. Amino acids critical for substrate affinity of rat organic cation transporter 1 line the substrate binding region in a model derived from the tertiary structure of lactose permease. *Mol Pharmacol* 2005;67:1600–11.

# Molecular Cancer Therapeutics

## Interactions of Tyrosine Kinase Inhibitors with Organic Cation Transporters and Multidrug and Toxic Compound Extrusion Proteins

Tsuyoshi Minematsu and Kathleen M. Giacomini

*Mol Cancer Ther* 2011;10:531-539. Published OnlineFirst January 20, 2011.

<b>Updated version</b>	Access the most recent version of this article at: doi: <a href="https://doi.org/10.1158/1535-7163.MCT-10-0731">10.1158/1535-7163.MCT-10-0731</a>
<b>Supplementary Material</b>	Access the most recent supplemental material at: <a href="http://mct.aacrjournals.org/content/suppl/2011/01/21/1535-7163.MCT-10-0731.DC1">http://mct.aacrjournals.org/content/suppl/2011/01/21/1535-7163.MCT-10-0731.DC1</a>

<b>Cited articles</b>	This article cites 44 articles, 20 of which you can access for free at: <a href="http://mct.aacrjournals.org/content/10/3/531.full#ref-list-1">http://mct.aacrjournals.org/content/10/3/531.full#ref-list-1</a>
<b>Citing articles</b>	This article has been cited by 21 HighWire-hosted articles. Access the articles at: <a href="http://mct.aacrjournals.org/content/10/3/531.full#related-urls">http://mct.aacrjournals.org/content/10/3/531.full#related-urls</a>

<b>E-mail alerts</b>	<a href="#">Sign up to receive free email-alerts</a> related to this article or journal.
<b>Reprints and Subscriptions</b>	To order reprints of this article or to subscribe to the journal, contact the AACR Publications Department at <a href="mailto:pubs@aacr.org">pubs@aacr.org</a> .
<b>Permissions</b>	To request permission to re-use all or part of this article, use this link <a href="http://mct.aacrjournals.org/content/10/3/531">http://mct.aacrjournals.org/content/10/3/531</a> . Click on "Request Permissions" which will take you to the Copyright Clearance Center's (CCC) Rightslink site.